Foot and Ankle Surgery 28 (2022) 919–927

Contents lists available at ScienceDirect

Foot and Ankle Surgery

journal homepage: www.journals.elsevier.com/foot-and-ankle-surgery

Semi-automatic software-based 3D-angular measurement for Weight-Bearing CT (WBCT) in the foot provides different angles than measurement by hand

Martinus Richter*, Fabian Duerr, Regina Schilke, Stefan Zech, Stefan Andreas Meissner, Issam Naef

Department for Foot and Ankle Surgery Rummelsberg and Nuremberg, Germany

ARTICLE INFO

Article history:
Received 7 October 2021
Received in revised form 28 December 2021
Accepted 6 January 2022

Keywords:
Weight-bearing CT
WBCT
Angle measurement
Semi-automatic measurement
Measurement by hand

ABSTRACT

Background: The purpose of this study was to compare semi-automatic software-based angular measurement (SAM) with previously validated measurement by hand (MBH) regarding angle values and time spent for the investigator for Weight-Bearing CT (WBCT).

Methods: In this retrospective comparative study, five-hundred bilateral WBCT scans (PedCAT, Curvebeam, Warrington, PA, USA) were included in the study. Five angles (1st - 2nd intermetatarsal angle (IM), talo-metatarsal 1-angle (TMT) dorsoplantar and lateral projection, hindfoot angle, calcaneal pitch angle) were measured with MBH and SAM (Bonelogic Ortho Foot and Ankle, Version 1.0.0-R, Disior Ltd, Helsinki, Finland) on the right/left foot/ankle. The angles and time spent of MBH and SAM were compared (t-test, homoscesdatic).

Results: The angles differed between MBH and SAM (mean values MBH/SAM; IM, 9.1/13.0; TMT dorsoplantar, −3.4/8.2; TMT lateral. −6.4/−1.1; hindfoot angle, 4.6/21.6; calcaneal pitch angle, 20.5/20.1; each $p < 0.001$ except the calcaneal pitch angle, $p = 0.35$). The time spent for MBH / SAM was 44.5 ± 12 s / 12 ± 0 s on average per angle ($p < 0.001$).

Conclusions: SAM provided different angles as MBH (except calcaneal pitch angle) and can currently not be considered as validated angle measurement method (except calcaneal pitch angle). The investigator time spent is 73% lower for SAM (12 s per angle) than for MBH (44.5 s per angle). SAM might be an important step forward for 3D-angle measurement of WBCT when valid angles are provided.

1. Introduction

Weight-bearing CT (WBCT) has been proven to allow for more precise and valid measurement of bone position (angles) than conventional weight-bearing radiographs (R) and conventional CT without weight-bearing (CT) [1–3]. The measurement by hand (MBH) has demonstrated adequate inter- and intraobserver reliability and validity but high time spent [1–3]. Therefore, the need for faster (semi-) automatic measurement was formulated [3]. Recently, a semi-automatic software-based angular measurement (SAM) has been developed (Bonelogic Ortho Foot and Ankle, Disior Ltd, Helsinki, Finland). The purpose of this study was to compare SAM with MBH regarding angles values and time spent for the investigator. The hypothesis was that there is no angle value difference between MBH and SAM.

2. Methods

In this retrospective comparative study, five-hundred bilateral WBCT scans (PedCAT, Curvebeam, Warrington, PA, USA) were randomly extracted from a local institutional database with more than 14,000 scans. No exclusion criteria such as metal implants were defined. The right or left foot/ankle was included in the study. The pathology was classified into the following groups: ankle osteoarthritis/instability, Haglund deformity/Achillodynia, forefoot deformity, Hallux rigidus, flatfoot, cavus foot, osteoarthritis except ankle. Five angles as shown in Table 1 were measured on single CT slices with MBH and SAM on the right foot/ankle [1,4,5].

* Correspondence to: Department for Foot and Ankle Surgery Rummelsberg and Nuremberg, Location Hospital Rummelsberg, Rummelsberg 71, 90592 Schwarzenbruck, Germany.
E-mail address: martinus.richter@sana.de (M. Richter).

https://doi.org/10.1016/j.fas.2022.01.001
1268-7731/

Table 1
Angles measurement by hand (MBH) versus semi-automatic measurement (SAM).

Parameter	MBH		SAM		t-test, p
	mean	STD	mean	STD	
IM-angle	9.1	3.5	13.0	3.7	< 0.001
TMT dorsoplantar	-3.4	12.0	8.2	12.6	< 0.001
TMT lateral	-6.4	9.2	-1.1	11.7	< 0.001
Hindfoot angle	4.6	7.5	21.6	6.4	< 0.001
Calcaneal pitch angle	20.5	5.4	20.1	5.3	0.34

IM, 1st - 2nd intermetatarsal angle; TMT, talo - 1st metatarsal - angle; STD, standard deviation.

2.1. Measurement by hand (MBH) [1]

The angles were digitally measured with specific software (Cubevue, version 3.7.0.3, Curvebeam, Warrington, USA).

The following angles were measured 1st - 2nd intermetatarsal angle, talo-metatarsal 1-angle (TMT) dorsoplantar and lateral projection, hindfoot angle, calcaneal pitch angle [1,6,7].

All bone axes (Tibia, talus, metatarsals) were defined as the straight line between the centers of the bones proximally and distally (epiphysis for distal tibia, and proximal and distal metatarsal) [1]. These bone centers were defined by linear measurements (Fig. 1a-d) [1].

The 1st - 2nd intermetatarsal angle was defined as the angle created between the axis of the 1st and the 2nd metatarsal in axial / horizontal reformation. The plane for the measurement was virtually rotated within the 3D-datase to achieve an exact congruency to the bone axes of 1st and 2nd metatarsals (Figs. 1a and 3a) [1].

The TMT angle was defined as the angle created between the axis of the 1st metatarsal and the talus (Fig. 1a and b) [1,6]. The dorsoplantar TMT angle was measured in the axial/horizontal reformation (Fig. 1b) [1]. The lateral TMT angle was measured in the parasagittal reformation (Figs. 1c and 3b) [1]. The plane for the measurement was virtually rotated within the 3D-datase to achieve an exact congruency to the bone axis of talus and 1st metatarsal [1]. The TMT angles were defined to be negative for abduction in the dorsoplantar radiograph and for dorsiflexion in the lateral radiographs [6].

The hindfoot angle was defined as the angle created between the axis of the distal tibia and the line between the center of the talar dome and the posterior calcaneal process (Figs. 1d and 3c) [1]. This angle was defined to be positive for hindfoot valgus and negative for hindfoot varus [1]. It was measured in the coronal reformation (Figs. 1d and 3c) [1]. The plane for the measurement was virtually rotated within the 3D-dataset to achieve an exact congruency to the bone axis of the tibia and the axis of the hindfoot (Fig. 1d) [1]. This was typically the case when this plane was congruent with the axis of the ankle, i.e. a line between medial and lateral malleolus comparable to a Mortise orientation but within a 3D-space [1]. Fig. 1d shows the orientation within the 3D dataset as described above with the adjusted rotation with the fibula and tibia aligned in the same virtual plane comparable to a Mortise view [1]. The calcaneal pitch angle was defined as the angle created between line between the lowest part of the posterior calcaneal process and the lowest part of

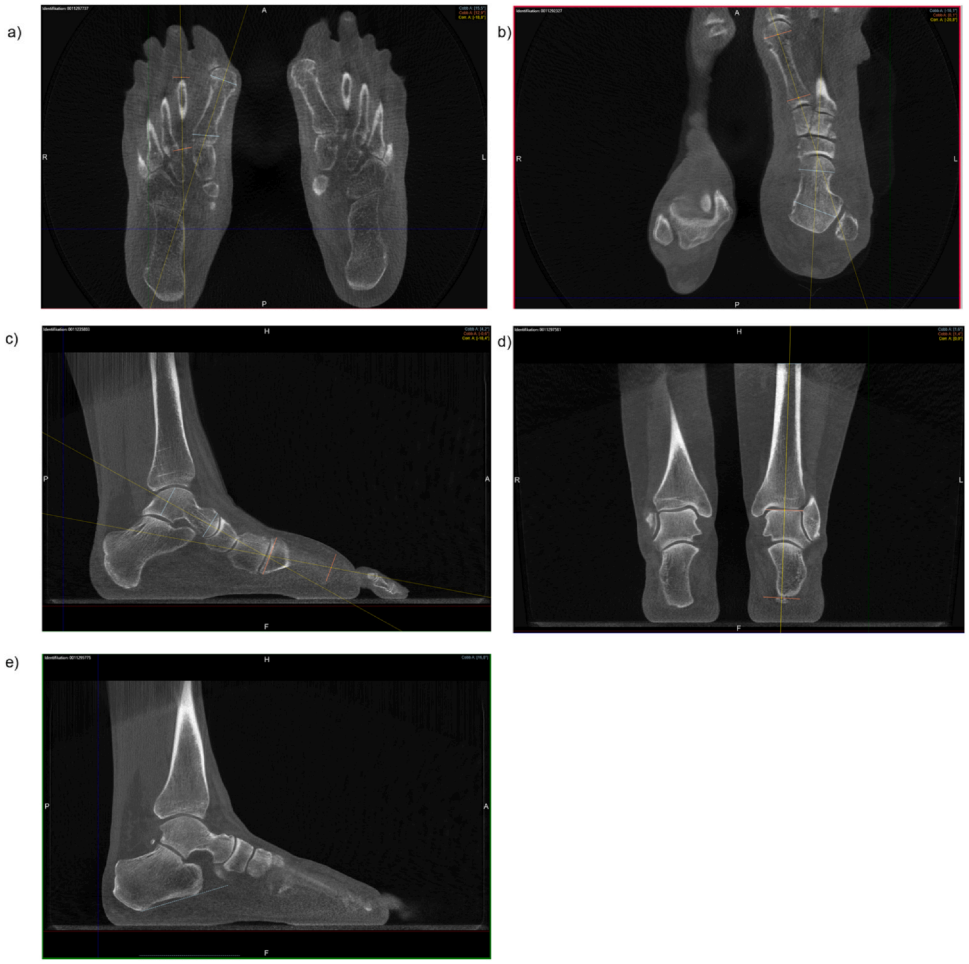

Fig. 1. a-e. Monitor views showing an example of some angle measurements by hand (Cubevue, version 3.7.0.3, Curvebeam, Warrington, USA). 1st - 2nd intermetatarsal angle (Fig. 1a), talo-metatarsal 1-angle (TMT) dorsoplantar (Fig. 1b) and lateral projection (Fig. 1c), hindfoot angle (Fig. 1d), and calcaneal pitch angle (Fig. 1e).

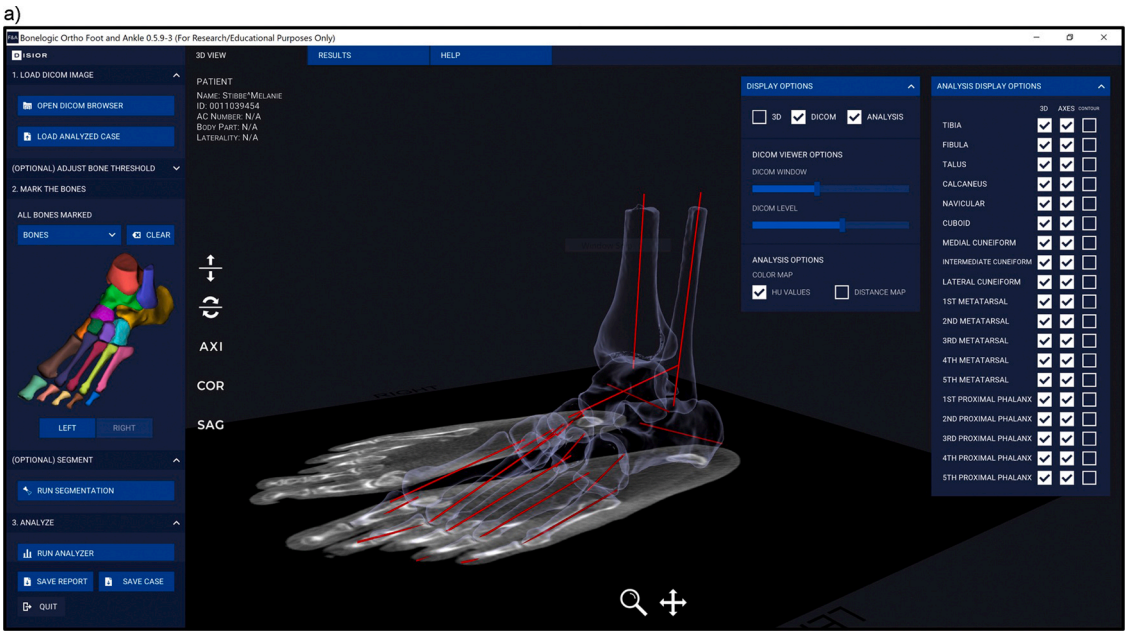

Fig. 2. a-f. Semi-automatic measurement software monitor view (Bonelogic Ortho Foot and Ankle, Version 1.0.0-R, Disior Ltd, Helsinki, Finland) (Fig. 2a). The software generates a 3D model with semi-automatic bone specification of tibia, fibula, talus, calcaneus, navicular, cuboid, cuneiforms, metatarsals and base phalanxes (Fig. 2a). The software automatically defines the longitudinal axes of these bones and automatically measures the angles between these axes: 1st - 2nd intermetatarsal angle (Fig. 2b), talo-metatarsal 1-angle (TMT) dorsoplantar (Fig. 2c) and lateral projection (Fig. 2d), and hindfoot angle (Fig. 2e). The calcaneal pitch angle was defined as the angle created between line between the lowest part of the posterior calcaneal process and the lowest part of the anterior calcaneal process, and a horizontal line (Fig. 2f).

the anterior calcaneal process, and a horizontal line. It was measured in the parasagittal reformation (Fig. 1e) [1]. The measurement was virtually rotated within the 3D-datase to achieve an exact congruency to an exactly parasagittal plane [1].

2.2. Semi-automatic measurement (SAM)

SAM includes software generated 3D models with semi-automatic bone specification of tibia, fibula, talus, calcaneus, navicular, cuboid, cuneiforms and metatarsals (Bonelogic Ortho Foot and Ankle, Version 1.0.0-R, Disior Ltd, Helsinki, Finland). Semi-automatic means that the investigator needs to define the different bones by mouse-click (Fig. 2a). The software automatically defines the longitudinal axes of these bones and automatically measures the angles between these axes: 1st - 2nd intermetatarsal angle (Figs. 2b and 3a), talo-metatarsal 1-angle (TMT) dorsoplantar (Fig. 2c) and lateral projection (Figs. 2d and 3c), and hindfoot angle (Figs. 2e and 3c). The calcaneal pitch angle was defined as the angle created between line between the lowest part of the posterior calcaneal process and the lowest part of the anterior calcaneal process, and a horizontal line (Fig. 2f). The methods for MBH as described above were forwarded to Disor to optimize the software to exactly mimic MBH.

2.3. Time spent

The time spent of the investigator for the measurements was recorded (total process MBH and specification of bones for SAM). The specification of bones during SAM took 60 s per foot and based on the further analysis of five angle a time spent of 12 s per angle was considered. Consequently, an analysis of 60 angles with SAM would have resulted in a calculated time spent of 1 s per angle. The software calculation time for SAM was not measured or considered as investigator time spent.

2.4. Statistics

IBM SPSS Statistics Version 25 (IBM, Armonk, NY, USA) was used for the statistical evaluation. The angles and time spent of MBH and SAM were compared (t-test, homoscedastic). The null hypothesis at a significant level of 0.05 was formulated that the different angles did not differ between the two methods. For non-significant findings, a power analysis was indicated. Sufficient power was defined as ≥ 0.8.

3. Results

3.1. Subjects

Mean age of the subject was 49 years (range, 18–85), 214 (43%) were male. The pathologies of the analyzed right feet were specified as follows; ankle osteoarthritis/instability, n = 147 (29%); Haglund deformity/Achillodynia, n = 41 (8%); forefoot deformity, n = 108 (22%); Hallux rigidus, n = 37 (7%); flatfoot, n = 35 (7%); cavus foot, n = 10 (2%); osteoarthritis except ankle, n = 82 (16%).

3.2. Angle measurement – differences between methods

The angles differed between MBH and SAM (each $p > 0.001$) except the calcaneal pitch angle ($p = 0.35$) (Table 1). The power was 0.91. Tables 2–4 show specific angles for different specific deformities (Forefoot, flatfoot, cavus foot). All angles differed between MBH and SAM except calcaneal pitch angles in flatfoot and cavus foot deformity and TMT dorsoplantar angles in cavus foot deformities. Table 5 shows the same analysis as Table 1 with absolute angle values. TMT dorsoplantar and lateral angles and calcaneal pith angles did not differ between MBH and SAM.

Fig. 2. (*continued*)

Fig. 2. (*continued*)

Fig. 2. (*continued*)

3.3. Time spent

The time spent for MBH / SAM was 44.5 ± 12 s / 12 ± 0 s on average per angle ($p < 0.001$).

4. Discussion

Most studies about WBCT focused on bone position measurement accuracy and/or pathology detection [1,8–60]. However, all these studies included MBH by investigators. Only Lintz et al. introduced an semiautomatic measurement method with the so-called Torque Ankle Lever Arm System (TALAS) [61]. SAM for commonly used angles as for example 1 s-2nd intermetatarsal angle in the 3D environment is available since 2020 but was not validated so far. We compared five angular measurements by hand that were validated before in 500 patient with SAM [1–3,62]. We expected that the artificial intelligence of SAM would provide valid angles, i.e. no differences with MBH. Contrary to our expectations, all angles measured with SAM differed significantly from MBH except calcaneal pitch angles. We were unsure if not the previously validated MBH could have been executed wrongly, and therefore performed a detailed qualitative analysis in cases with different angular measurement results as shown in Fig. 3a-3c. The angles are not very different but also not accurate. Our results are in contrast to the findings or Day et al. regarding automatic measurement of 1st-2nd intermetatarsal angle. They observed accurate and reliable SAM in 128 feet in 93 patients with the same method we used [62]. Ortolani et al. found also less differences between MBH and SAM [63]. These studies and cases from our study with correct SAM angles in combination with almost no time spent showed the real potential of SAM. The SAM system will have to become reliable and valid which has to be proven by further studies in the future. One could argue that also MBH might result in different values when repetitively measured as shown in the initial validation studies [1,2]. SAM measured the calcaneal pitch angles exactly as MBH which also proves that MBH is a reliably measurement. The 1st - 2nd intermetatarsal angles with MBH was 9.1° on average and with SAM 13.0°, i.e. 3.9° or 43% more ($p < 0.001$). One could not argue that this difference is clinically not relevant or that SAM was still somehow good enough despite significant differences in comparison with MHB as for the calcaneal pitch angle. The same for the hindfoot angles with 4.6° on average with MBH and 21.6°, i.e. 16.8° or 365% more on average with SAM. 1st - 2nd intermetatarsal angles and hindfoot angles were at least the same principal direction relating positive and negative. A positive hindfoot angle reflects hindfoot valgus and MBH and SAM resulted both in positive values. This was not the case for the talo - 1st metatarsal - angles (TMT). TMT dorsoplantar and lateral were negative with MBH (−3.4°/−6.4°) but positive with SAM (8.1°/9.2°) on average. This means that the measurements with MBH resulted in midfoot/forefoot dorsiflexion respectively flatfoot (negative TMT lateral) and midfoot/forefoot abduction (negative TMT dorsoplantar). In contrast, the measurements with SAM resulted in midfoot/forefoot plantiflexion respectively cavus foot (positive TMT lateral) and midfoot/forefoot adduction (positive TMT dorsoplantar). This means (approved by a qualitative case-to-case-analysis) that SAM cannot correctly diminish between flatfoot/cavus foot and midfoot/forefoot ab-/adduction. When looking into specific deformities and specific angles, the situation changes a little. The 1st - 2nd intermetatarsal angles did still differ between MBH and SAM in forefoot deformities (n = 108) (Table 2). In flatfoot deformities (n = 35), the calcaneal pitch angles did not differ between MBH and SAM but TMT dorsoplantar and lateral angles and hindfoot angles did still differ (Table 3). In hindfoot deformities (n = 10), the calcaneal pitch angles and TMT

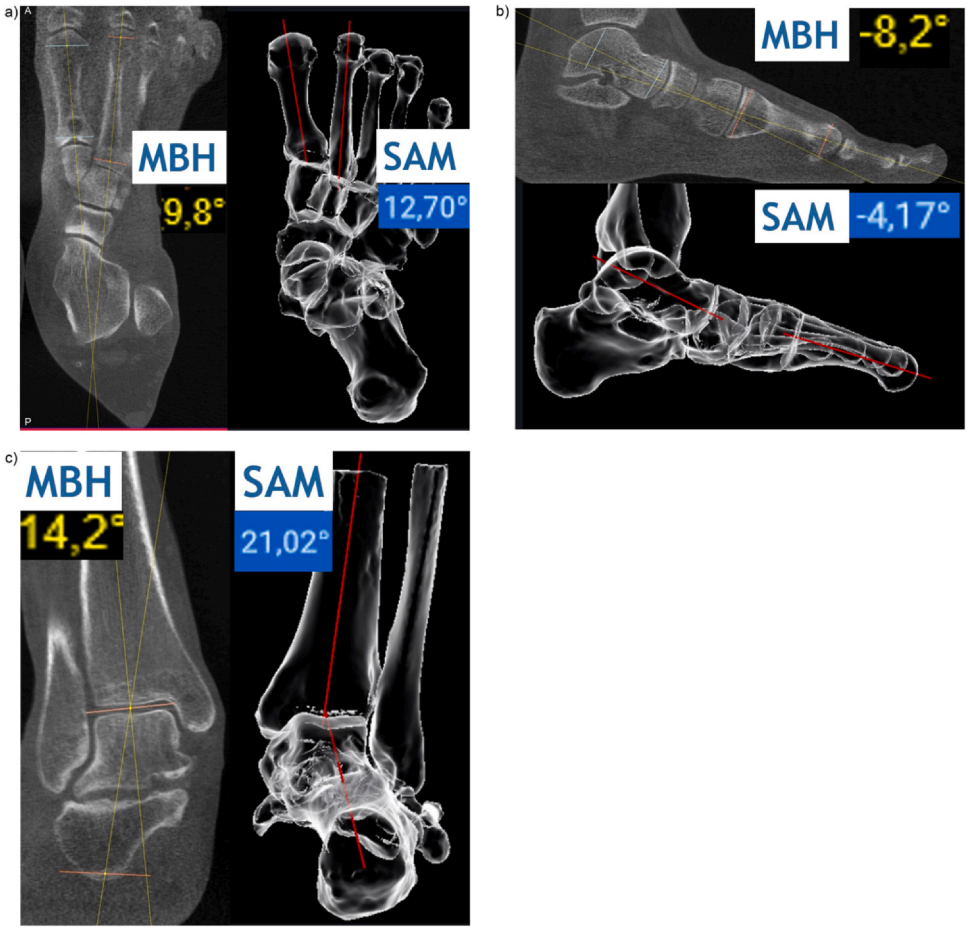

Fig. 3. a-c. Comparison measurements by hand (MBH) with semi-automatic measurement (SAM) 1st - 2nd intermetatarsal angle (Fig. 3a), talo-metatarsal 1-angle (TMT) lateral projection (Fig. 3b), and hindfoot angle (Fig. 3c) in different feet. The angle values are shown as provided by the measurement software as described in Figs. 1 and 2. The 1st - 2nd intermetatarsal angle (Fig. 3a) was 9.8° provided with MBH and 12.7° with SAM. The talo-metatarsal 1-angle (TMT) lateral projection (Fig. 3b) was − 8.2° provided with MBH and − 4.17° with SAM. The hindfoot angle (Fig. 3c) was 14.2° provided with MBH and 21.02° with SAM.

Table 2
Angles measurement by hand (MBH) versus semi-automatic measurement (SAM) in cases with forefoot deformity (n = 108).

Parameter	MBH		AM		t-test, p
	mean	STD	mean	STD	
IM-angle	10.7	3.8	14.3	3.9	< 0.001

IM, 1st - 2nd intermetatarsal angle; STD, standard deviation.

Table 3
Angles measurement by hand (MBH) versus semi-automatic measurement (SAM) with flatfoot deformity (n = 35).

Parameter	MBH		AM		t-test, p
	mean	STD	mean	STD	
TMT dorsoplantar	-15.3	12.6	21.3	13.1	< 0.001
TMT lateral	-16.8	6.6	-11.2	10.7	0.01
Hindfoot angle	13.1	6.0	26.9	5.2	< 0.001
Calcaneal pitch angle	17.1	6.8	16.8	6.3	0.873

TMT, talo - 1st metatarsal - angle; STD, standard deviation.

lateral angles did not differ between MBH and SAM but TMT dorsoplantar angles and hindfoot angles did still differ (Table 4). However, the statistical power of this deformity specific analysis was only sufficient for forefoot deformities, i.e. the missing differences in some angles might be caused by too low case numbers. One issue could be that SAM was just not able to determine negative angle values. We therefore analyzed also absolute values (without +/-)

Table 4
Angles measurement by hand (MBH) versus semi-automatic measurement (AM) with Cavus foot deformity (n = 10).

Parameter	MBH		AM		t-test, p
	mean	STD	mean	STD	
TMT dorsoplantar	15.5	16.0	-14.7	12.4	< 0.001
TMT lateral	6.5	10.0	14.5	9.5	0.081
Hindfoot angle	-9.6	6.4	10.0	7.6	< 0.001
Calcaneal pitch angle	24.5	4.2	25.2	5.2	0.721

TMT, talo - 1st metatarsal - angle; STD, standard deviation.

Table 5
Angles measurement by hand (MBH) versus semi-automatic measurement (SAM) entire population (n = 500) with absolute values.

Parameter	MBH		AM		t-test, p
	mean	STD	mean	STD	
IM-angle	9.1	3.5	12.0	3.7	< 0.001
TMT dorsoplantar	9.7	7.9	12.1	8.9	0.067
TMT lateral	8.9	6.9	9.0	7.5	0.726
Hindfoot angle	7.0	5.2	21.6	6.2	< 0.001
Calcaneal pitch angle	20.4	5.4	20.1	5.3	0.347

IM, 1st - 2nd intermetatarsal angle; TMT, talo - 1st metatarsal - angle; STD, standard deviation.

(Table 5). However, this did not change the significances for 1st - 2nd intermetatarsal angles, hindfoot angles and calcaneal pitch angles. Interestingly, TMT dorsoplantar and lateral angles did not differ

between MBH and SAM despite sufficient statistical power. It seems that the insufficient detection of negative has partly caused the significances. This is of theoretical value because a method that is not able to diminish between positive and negative angles would not be useful and never valid.

4.1. Shortcomings of the study

Potential shortcomings of the study are low case number and questionable validity of MBH. Five measured angles in 500 feet sums up to 2,500 angles in addition to highly significant differences between measurement types ensures adequate case number. MBH as used in this study was performed exactly as used before [1,2]. In these earlier studies, MBH showed excellent intra- and interobserver reliability, and adequate validity was therefore concluded [1,2]. One could argue that high intra- and interobserver reliability does not ensure adequate validity as discussed before [1,2]. A qualitative analysis as performed in this study supported also the validity of MBH.

In conclusion, SAM provided different angles as MBH (except calcaneal pitch angle) and can currently not be considered as validated angle measurement method (except calcaneal pitch angle). The investigator time spent is 73% lower for SAM (12 s per angle) than for MBH (44.5 s per angle). Cases with correct angles in combination with almost no time spent show the real potential of SAM. The SAM system will have to become reliable and valid which has to be proven by further studies in the future.

Conflict of interest statement

None of the authors or the authors´ institution received funding in relation to this study. The first and corresponding author is consultant of Curvebeam, Geistlich, Iintercus, Ossio and Iimplants International, proprietor of R-Innovation, and shareholder of Curvebeam.

References

[1] Richter M, Seidl B, Zech S, Hahn S. PedCAT for 3D-imaging in standing position allows for more accurate bone position (angle) measurement than radiographs or CT. Foot Ankle Surg 2014;20:201–7.
[2] Richter M, Zech S, Hahn S, Naef I, Merschin D. Combination of pedCAT for 3D imaging in standing position with pedography shows no statistical correlation of bone position with force/pressure distribution. J Foot Ankle Surg 2016;55(2):240–6.
[3] Richter M, Lintz F, Cesar de Netto C, Barg A, Burssens A, Ellis S. Weight Bering Cone Beam Computed Tomography (WBCT) in the Foot and Ankle: A Scientific, Technical and Clinical Guide. Cham: Springer Nature Switzerland AG,; 2020.
[4] Richter M, Lintz F, de Cesar Netto C, Barg A, Burssens A. Results of more than 11,000 scans with weightbearing CT – impact on costs, radiation exposure, and procedure time. Foot Ankle Surg 2020;26(5):518–22.
[5] Richter M, Lintz F, Cesar de Netto C, Barg A, Burssens A, Ellis S. Results of a 6.8 year, 13,000 scans experience with Weight-Bearing CT. Impact on costs, radiation exposure and time spent. Fuss Sprungg 2020;18:185–92.
[6] Richter M, Zech S. Lengthening osteotomy of the calcaneus and flexor digitorum longus tendon transfer in flexible flatfoot deformity improves Talo-1st metatarsal-index, clinical outcome and pedographic parameter. Foot Ankle Surg 2012;19(1):56–61.
[7] Saltzman CL, el-Khoury GY. The hindfoot alignment view. Foot Ankle Int 1995;16(9):572–6.
[8] Zhang JZ, Lintz F, Bernasconi A, Zhang S. 3D biometrics for hindfoot alignment using weightbearing computed tomography. Foot Ankle Int 2019:684–9.
[9] Welck MJ, Myerson MS. The value of Weight-Bearing CT scan in the evaluation of subtalar distraction bone block arthrodesis: case report. Foot Ankle Surg 2015;21(4):e55–9.
[10] Tuominen EK, Kankare J, Koskinen SK, Mattila KT. Weight-bearing CT imaging of the lower extremity. AJR Am J Roentgenol 2013;200(1):146–8.
[11] Richter M, Lintz F, Zech S, Meissner SA. Combination of PedCAT weightbearing CT with pedography assessment of the relationship between anatomy-based foot center and force/pressure-based center of gravity. Foot Ankle Int 2018;39(3):361–8.
[12] Lintz F, Welck M, Bernasconi A, Thornton J, Cullen NP, Singh D, et al. 3D biometrics for hindfoot alignment using weightbearing CT. Foot Ankle Int 2017;38(6):684–9.
[13] Lepojarvi S, Niinimaki J, Pakarinen H, Leskela HV. Rotational dynamics of the normal distal tibiofibular joint with weight-bearing computed tomography. Foot Ankle Int 2016;37(6):627–35.
[14] Lepojarvi S, Niinimaki J, Pakarinen H, Koskela L, Leskela HV. Rotational dynamics of the talus in a normal tibiotalar joint as shown by weight-bearing computed tomography. J Bone Jt Surg Am 2016;98(7):568–75.
[15] Lawlor MC, Kluczynski MA, Marzo JM. Weight-bearing cone-beam CT scan assessment of stability of supination external rotation ankle fractures in a Cadaver model. Foot Ankle Int 2018;39(7):850–7.
[16] Krahenbuhl N, Tschuck M, Bolliger L, Hintermann B, Knupp M. Orientation of the subtalar joint: measurement and reliability using weightbearing CT scans. Foot Ankle Int 2016;37(1):109–14.
[17] Jeng CL, Rutherford T, Hull MG, Cerrato RA, Campbell JT. Assessment of bony subfibular impingement in flatfoot patients using weight-bearing CT scans. Foot Ankle Int 2019;40(2):152–8.
[18] Hirschmann A, Pfirrmann CW, Klammer G, Espinosa N, Buck FM. Upright cone CT of the hindfoot: comparison of the non-weight-bearing with the upright weight-bearing position. Eur Radiol 2014;24(3):553–8.
[19] Ferri M, Scharfenberger AV, Goplen G, Daniels TR, Pearce D. Weightbearing CT scan of severe flexible pes planus deformities. Foot Ankle Int 2008;29(2):199–204.
[20] de Cesar Netto C, Schon LC, Thawait GK, da Fonseca LF, Chinanuvathana A, Zbijewski WB, et al. Flexible adult acquired flatfoot deformity: comparison between weight-bearing and non-weight-bearing measurements using cone-beam computed tomography. J Bone Jt Surg Am 2017;99(18):e98.
[21] Collan L, Kankare JA, Mattila K. The biomechanics of the first metatarsal bone in hallux valgus: a preliminary study utilizing a weight bearing extremity CT. Foot Ankle Surg 2013;19(3):155–61.
[22] Colin F, Horn Lang T, Zwicky L, Hintermann B, Knupp M. Subtalar joint configuration on weightbearing CT scan. Foot Ankle Int 2014;35(10):1057–62.
[23] Burssens A, Peeters J, Peiffer M, Marien R, Lenaerts T, Vandeputte G, et al. Reliability and correlation analysis of computed methods to convert conventional 2D radiological hindfoot measurements to a 3D setting using weight-bearing CT. Int J Comput Assist Radiol Surg 2018;13(12):1999–2008.
[24] Burssens A, Peeters J, Buedts K, Victor J, Vandeputte G. Measuring hindfoot alignment in weight bearing CT: a novel clinical relevant measurement method. Foot Ankle Surg 2016;22(4):233–8.
[25] Barg A, Bailey T, Richter M, de Cesar Netto C, Lintz F, Burssens A, et al. Weightbearing computed tomography of the foot and ankle: emerging technology topical review. Foot Ankle Int 2018;39(3):376–86.
[26] An TW, Michalski M, Jansson K, Pfeffer G. Comparison of lateralizing calcaneal osteotomies for varus hindfoot correction. Foot Ankle Int 2018;39(10):1229–36.
[27] Zhang Y, Xu J, Wang X, Huang J, Zhang C, Chen L, et al. An in vivo study of hindfoot 3D kinetics in stage II posterior tibial tendon dysfunction (PTTD) flatfoot based on weight-bearing CT scan. Bone Jt Res 2013;2(12):255–63.
[28] Yoshioka N, Ikoma K, Kido M, Imai K, Maki M, Arai Y, et al. Weight-bearing three-dimensional computed tomography analysis of the forefoot in patients with flatfoot deformity. J Orthop Sci 2016;21(2):154–8.
[29] Welck MJ, Singh D, Cullen N, Goldberg A. Evaluation of the 1st metatarso-sesamoid joint using standing CT – the Stanmore classification. Foot Ankle Surg 2018;24(4):314–9.
[30] Thawait GK, Demehri S, AlMuhit A, Zbijweski W, Yorkston J, Del Grande F, et al. Extremity cone-beam CT for evaluation of medial tibiofemoral osteoarthritis: initial experience in imaging of the weight-bearing and non-weight-bearing knee. Eur J Radiol 2015;84(12):2564–70.
[31] Segal NA, Nevitt MC, Lynch JA, Niu J, Torner JC, Guermazi A. Diagnostic performance of 3D standing CT imaging for detection of knee osteoarthritis features. Physician Sportsmed 2015;43(3):213–20.
[32] Segal NA, Frick E, Duryea J, Roemer F, Guermazi A, Nevitt MC, et al. Correlations of medial joint space width on fixed-flexed standing computed tomography and radiographs with cartilage and meniscal morphology on magnetic resonance imaging. Arthritis Care Res 2016;68(10):1410–6.
[33] Segal NA, Frick E, Duryea J, Nevitt MC, Niu J, Torner JC, et al. Comparison of tibiofemoral joint space width measurements from standing CT and fixed flexion radiography. J Orthop Res 2017;35(7):1388–95.
[34] Segal NA, Bergin J, Kern A, Findlay C, Anderson DD. Test-retest reliability of tibiofemoral joint space width measurements made using a low-dose standing CT scanner. Skelet Radiol 2017;46(2):217–22.
[35] Marzo JM, Kluczynski MA, Clyde C, Anders MJ, Mutty CE, Ritter CA. Weight bearing cone beam CT scan versus gravity stress radiography for analysis of supination external rotation injuries of the ankle. Quant Imaging Med Surg 2017;7(6):678–84.
[36] Marzo J, Kluczynski M, Notino A, Bisson L. Comparison of a novel weightbearing cone beam computed tomography scanner versus a conventional computed tomography scanner for measuring patellar instability. Orthop J Sports Med 2016;4(12):1–7.
[37] Lintz F, de Cesar Netto C, Barg A, Burssens A, Richter M. Weight-bearing cone beam CT scans in the foot and ankle. EFORT Open Rev 2018;3(5):278–86.
[38] Kunas GC, Probasco W, Haleem AM, Burket JC, Williamson ERC, Ellis SJ. Evaluation of peritalar subluxation in adult acquired flatfoot deformity using computed tomography and weightbearing multiplanar imaging. Foot Ankle Surg 2018;24(6):495–500.
[39] Kimura T, Kubota M, Taguchi T, Suzuki N, Hattori A, Marumo K. Evaluation of first-ray mobility in patients with hallux valgus using weight-bearing CT and a 3-D analysis system: a comparison with normal feet. J Bone Jt Surg Am 2017;99(3):247–55.

[40] Kimura T, Kubota M, Suzuki N, Hattori A, Marumo K. Comparison of intercuneiform 1-2 joint mobility between hallux valgus and normal feet using weightbearing computed tomography and 3-dimensional analysis. Foot Ankle Int 2018;39(3):355–60.
[41] Kim JB, Yi Y, Kim JY, Cho JH, Kwon MS, Choi SH, et al. Weight-bearing computed tomography findings in varus ankle osteoarthritis: abnormal internal rotation of the talus in the axial plane. Skelet Radiol 2017;46(8):1071–80.
[42] Hoogervorst P, Working ZM, El Naga AN, Marmor M. In vivo CT analysis of physiological fibular motion at the level of the ankle syndesmosis during plantigrade weight bearing. Foot Ankle Spec 2019;12(3):233–7. https://doi.org/10.1177/1938640018782602
[43] Godoy-Santos AL, Cesar CN. Weight-bearing computed tomography of the foot and ankle: an update and future directions. Acta Ortop Bras 2018;26(2):135–9.
[44] Cody EA, Williamson ER, Burket JC, Deland JT, Ellis SJ. Correlation of talar anatomy and subtalar joint alignment on weightbearing computed tomography with radiographic flatfoot parameters. Foot Ankle Int 2016;37(8):874–81.
[45] Cheung ZB, Myerson MS, Tracey J, Vulcano E. Weightbearing CT scan assessment of foot alignment in patients with hallux rigidus. Foot Ankle Int 2018;39(1):67–74.
[46] Burssens A, Van Herzele E, Leenders T, Clockaerts S, Buedts K, Vandeputte G, et al. Weightbearing CT in normal hindfoot alignment – constitutional valgus? Foot Ankle Surg 2018;24(3):213–8.
[47] Shakoor D, Osgood GM, Brehler M, Zbijewski WB, de Cesar Netto C, Shafiq B, et al. Cone-beam CT measurements of distal tibio-fibular syndesmosis in asymptomatic uninjured ankles: does weight-bearing matter? Skelet Radiol 2019;48(4):583–94.
[48] Patel S, Malhotra K, Cullen NP, Singh D, Goldberg AJ, Welck MJ. Defining reference values for the normal tibiofibular syndesmosis in adults using weight-bearing CT. Bone Jt J 2019;101-b(3):348–52.
[49] Osgood GM, Shakoor D, Orapin J, Qin J, Khodarahmi I, Thawait GK, et al. Reliability of distal tibio-fibular syndesmotic instability measurements using weightbearing and non-weightbearing cone-beam CT. Foot Ankle Surg 2018. https://doi.org/10.1016/j.fas.2018.10.003. ([Epub ahead of print]).
[50] Malhotra K, Welck M, Cullen N, Singh D, Goldberg AJ. The effects of weight bearing on the distal tibiofibular syndesmosis: a study comparing weight bearing-CT with conventional CT. Foot Ankle Surg 2019;25(4):511–6. https://doi.org/10.1016/j.fas.2018.03.006. ([Epub ahead of print]).
[51] Lintz F, de Cesar Netto C, Burssens A, Barg A, Richter M. The value of axial loading three dimensional (3D) CT as a substitute for full weightbearing (standing) 3D CT: comparison of reproducibility according to degree of load. Foot Ankle Surg 2018;24(6):553–4.
[52] Krahenbuhl N, Bailey TL, Weinberg MW, Davidson NP, Hintermann B, Presson AP, et al. Impact of torque on assessment of syndesmotic injuries using weightbearing computed tomography scans. Foot Ankle Int 2019;40(5):710–9.
[53] Krahenbuhl N, Bailey TL, Presson AP, Allen CM, Henninger HB, Saltzman CL, et al. Torque application helps to diagnose incomplete syndesmotic injuries using weight-bearing computed tomography images. Skelet Radiol 2019;48(9):1367–76.
[54] Kleipool RP, Dahmen J, Vuurberg G, Oostra RJ, Blankevoort L, Knupp M, et al. Study on the three-dimensional orientation of the posterior facet of the subtalar joint using simulated weight-bearing CT. J Orthop Res 2019;37(1):197–204.
[55] Kennelly H, Klaassen K, Heitman D, Youngberg R, Platt SR. Utility of weight-bearing radiographs compared to computed tomography scan for the diagnosis of subtle Lisfranc injuries in the emergency setting. Emerg Med Austral: EMA 2019;31(5):741–4. https://doi.org/10.1111/742-6723.13237
[56] Ha AS, Cunningham SX, Leung AS, Favinger JL, Hippe DS. Weightbearing digital tomosynthesis of foot and ankle arthritis: comparison with radiography and simulated weightbearing CT in a prospective study. AJR Am J Roentgenol 2019;212(1):173–9.
[57] de Cesar Netto C, Shakoor D, Roberts L, Chinanuvathana A, Mousavian A, Lintz F, et al. Hindfoot alignment of adult acquired flatfoot deformity: a comparison of clinical assessment and weightbearing cone beam CT examinations. Foot Ankle Surg 2019;25(6):790–7.
[58] de Cesar Netto C, Shakoor D, Dein EJ, Zhang H, Thawait GK, Richter M, et al. Influence of investigator experience on reliability of adult acquired flatfoot deformity measurements using weightbearing computed tomography. Foot Ankle Surg 2019;25(4):495–592.
[59] de Cesar Netto C, Bernasconi A, Roberts L, Pontin PA, Lintz F, Saito GH, et al. Foot alignment in symptomatic national basketball association players using weightbearing cone beam computed tomography. Orthop J Sports Med 2019;7(2). https://doi.org/10.1177/2325967119826081
[60] Burssens A, Vermue H, Barg A, Krahenbuhl N, Victor J, Buedts K. Templating of syndesmotic ankle lesions by use of 3D analysis in weightbearing and non-weightbearing CT. Foot Ankle Int 2018;39(12):1487–96.
[61] Lintz F, Welck M, Bernasconi A, Thornton BJ, Cullen NP, Singh D, et al. 3D biometrics for hindfoot alignment using weightbearing CT. Foot Ankle Int 2017;38(6):684–9. 1071100717690806.
[62] Day J, de Cesar Netto C, Richter M, Mansur NS, Fernando C, Deland JT, et al. Evaluation of a weightbearing CT artificial intelligence-based automatic measurement for the M1-M2 intermetatarsal angle in hallux valgus. Foot Ankle Int 2021:10711007211015177.
[63] Ortolani M, Leardini A, Pavani C, Scicolone S, Girolami M, Bevoni R, et al. Angular and linear measurements of adult flexible flatfoot via weight-bearing CT scans and 3D bone reconstruction tools. Sci Rep 2021;11(1):16139.